

0038-1098(94)E0119-V

Raman Studies of Doped Polycrystalline Silicon From Laser-Annealed, Doped a-Si:H

A. Compaan, M. E. Savage,

Dept. of Physics and Astronomy, The University of Toledo, Toledo, OH 43606, USA

A. Aydinli, and T. Azfar

Dept. of Physics, Bilkent University, Ankara 06533, Turkey

(Received 22 December 1993 by M. Cardona)

(Received form 20 January 1994)

We have used Raman scattering to follow the progress of multiple-pulse (sub-melt-threshold) laser annealing in doped hydrogenated amorphous silicon films (a-Si:H) on glass. In phosphorous-doped a-Si:H the Raman signal shows that recrystallization begins with the first laser pulse but that multiple pulses are needed to generate the highest hole concentrations of $\sim 6 \times 10^{20} \text{ cm}^{-3}$. In boron-doped a-Si:H the electron concentration reaches $\sim 1 \times 10^{21} \text{ cm}^{-3}$ after laser anneal which produces a dip rather than a peak near the phonon line as a consequence of a negative Fano-interference parameter, q . The results show that Raman scattering can be used to obtain carrier concentrations in poly-silicon provided that wavelength-dependent Fano interference effects are properly included.

In doped Si, free particle scattering interferes with the discrete phonon Raman scattering to produce asymmetric and broadened lineshapes. This Fano lineshape has been studied extensively in heavily-doped crystalline Si^{1,2} including pulsed-laser-annealed, ion-implanted layers³ but has not been examined in the extremely heavily doped poly-Si which can be prepared by pulsed laser recrystallization of hydrogenated amorphous silicon (a-Si:H).^{4,5} In this communication we examine the Raman lineshape in heavily doped polycrystalline silicon thin films prepared by pulsed excimer laser annealing of doped a-Si:H thin films grown by plasma-enhanced chemical vapor deposition on glass substrates.⁶ In fact the laser-annealed thin films on glass, in spite of their polycrystallinity, present some advantage for such a study because of the absence of strong scattering from the Si substrate which can obscure some of the features in pulsed-laser-annealed ion-implanted epitaxial layers.

The linewidth and asymmetry of phonon Raman lines has also been used to obtain grain sizes in undoped polycrystalline semiconductors. In this case, the asymmetry arises from the relaxation of wavevector selection rules due to finite wavevector effects in very small crystallites ($\leq 100 \text{ \AA}$). This technique was first used in undoped polycrystalline silicon thin films⁷ and has subsequently been extended to several other semiconductor systems and also applied to the case of alloy broadening and ion-implantation-produced damage effects.⁸ However, doped semiconductors can present problems for such lineshape analyses due to line shape changes and broadening arising from effects of single particle scattering from free carriers. Understanding the various contributions to the Raman line shift and shape can improve the utility of Raman scattering as a tool to obtain carrier concentrations. This is

particularly useful in polycrystalline materials where transport measurements are complicated by grain boundary effects. Transport properties of doped polycrystalline Si are of considerable interest due the material's use in photovoltaics and thin-film transistors.⁹

Previous studies of pulsed-laser-annealed films of undoped a-Si:H have shown that a layered structure exists after annealing. Annealing with a picosecond YAG laser⁵ and with 10-20 nsec excimer lasers⁶ have been shown to form a thin (30 - 100 nm) surface layer which is polycrystalline (grain sizes $\geq 50 \text{ nm}$). Underneath this lies a microcrystalline or fine-grained layer (usually observed as a region with grains of 20 nm diameter or less surrounded by amorphous material^{4,10}) of about the same thickness. In addition the laser annealing may produce a layer of a-Si with greatly reduced hydrogen content immediately under the microcrystalline Si. Finally, if the original films are thick enough, there may remain a residual layer of unannealed a-Si:H. We shall use this four-layer model⁴ to interpret our Raman data.

The Raman scattering was performed with two argon laser lines ($\lambda = 457.9 \text{ nm}$ and 514.5 nm) and the krypton laser line at $\lambda = 647.1 \text{ nm}$ using a cylindrical focus to avoid beam heating effects. The power density on the sample was below 10 W/cm^2 . The Raman spectra obtained at Toledo utilized an ISA S3000 triple spectrometer operated in the scanning mode, whereas the data obtained at Bilkent used a JY U1000 double spectrometer. All data were obtained at room temperature with the samples held in air. The Raman probe depths for backscattering [$(2\alpha)^{-1}$, where α is the absorption coefficient] in crystalline or polycrystalline Si are $0.15 \text{ }\mu\text{m}$ for $\lambda=458 \text{ nm}$, $0.30 \text{ }\mu\text{m}$ for 514 nm , and $1.5 \text{ }\mu\text{m}$ for 647 nm .

n-type films--The progress of sub-melt-threshold

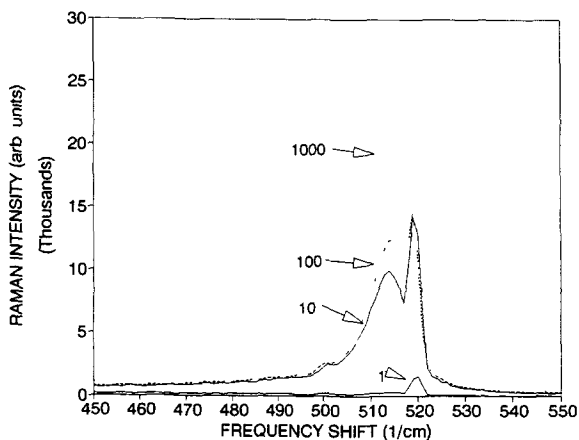


Fig. 1: Raman scattering at $\lambda = 514.5$ nm from phosphorous-doped a-Si:H (n-type) films after 1, 10, 100, and 1000 XeCl laser pulses at 150 mJ/cm^2 .

laser annealing with increasing numbers of laser pulses in P-doped a-Si:H is shown in Figure 1. With the pulse energy density of 150 mJ/cm^2 , one annealing pulse produces a distinct peak near 520 cm^{-1} corresponding to the Raman-active (Brillouin-zone-center) mode $\Gamma_{25'}$ in crystalline Si. However, with 10, 100, and 1000 pulses, a second peak develops which is shifted downward by $\sim 4.5 \pm 0.5 \text{ cm}^{-1}$. It is also broader and asymmetric.

Although asymmetry may arise from microcrystallinity due to relaxation of crystal momentum selection rules,⁷ this grain size effect is not the cause of the observed broadening in these phosphorous-doped samples. This is confirmed by comparison with similar data obtained on annealed, undoped a-Si:H as shown in Fig. 2a. In this case we have laser annealed a similar, but undoped a-Si:H film. Similar annealing behavior is observed but in this case the

Raman line does not shift to lower frequencies after additional pulses. (The annealing pulse energy for the undoped film was 300 mJ/cm^2 , consistent with the previously observed higher threshold for multiple-pulse annealing of undoped films.)⁵

The shift, broadening, and asymmetry of this second peak in annealed a-Si:H:P films is a result of improved carrier activation with additional pulses. These are characteristic signatures in Raman scattering of n-type electrical activation of the phosphorous dopants. The amount of asymmetry and phonon softening (downward frequency renormalization) increases with dopant concentration.

The effects of n-type doping on the Raman spectra from crystalline Si have been reviewed by Abstreiter and Cardona¹¹ and the frequency shift in extremely heavily doped crystalline Si has been measured in Raman scattering by Compaan, Contreras, and Cardona³ For the case of heavily doped n-Si, the continuum of single-particle excitations which interferes with the discrete phonon line arises from inelastic scattering of electrons near the X-point of the conduction band. In general the peak shift and line shape can be used to estimate the doping density. From the shift of $4.5 \pm 0.5 \text{ cm}^{-1}$ observed in Fig. 1 and by comparison with the data of Ref. 3, we infer that the electron concentration is $6 \pm 2 \times 10^{20} \text{ cm}^{-3}$.

There are two plausible models for the mixture of doped and undoped material implied by the double peak in the Raman scattering. The annealed polycrystalline material may have some grains with few free carriers and others with a high density of free carriers and additional laser pulses simply increase the number of grains or fraction of material with high carrier density. Alternatively the low activation region may be confined to a layer below the region of high carrier activation. The spectra of Fig. 1 do not directly yield an interpretation. However spectra obtained at $\lambda=457.9 \text{ nm}$ (Fig. 2b) provide the answer. The Raman probe depth at 457.9 nm is only $\sim 0.15 \mu\text{m}$, whereas

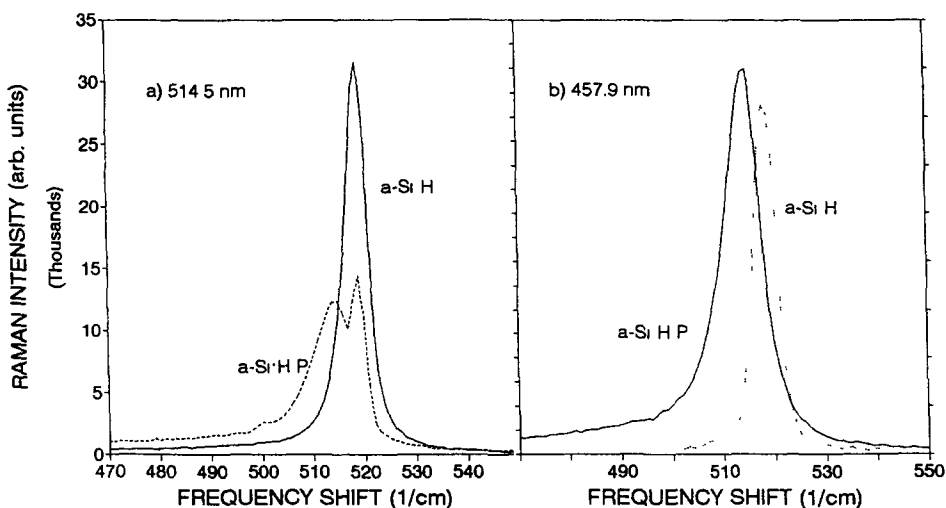


Fig. 2: Comparison of Raman scattering from phosphorous-doped a-Si:H film after 1000 laser pulses at 150 mJ/cm^2 and undoped a-Si:H after 1000 pulses at 300 mJ/cm^2 . a) $\lambda=514.5 \text{ nm}$; b) $\lambda=457.9 \text{ nm}$.

at 514.5 nm it is 0.30 μm . Fig. 2b shows that the unshifted Raman line at 520 cm^{-1} is absent with 457.9 nm excitation. This indicates that the region of low carrier activation lies beyond the range of the 457.9 nm beam or approximately 0.3 μm below the surface.

Our interpretation is that in the initial stages of laser annealing (first few pulses), recrystallization occurs with the associated evolution of hydrogen from the film. However, the initial crystallites must possess sufficiently high numbers of defects that carrier activation is suppressed. Incomplete H evolution could be a factor leading to suppression of dopant activity. Further annealing with additional pulses removes carrier traps and activates the dopants. The Raman data show that even after 1000 pulses a recrystallized but electrically inactive layer persists deep in the film, presumably near the boundary with the microcrystalline and/or amorphous material. This boundary layer is simply driven deeper and deeper into the film with increasing numbers of pulses.

p-type films—Pulsed laser annealing of boron-doped a-Si:H yields extremely heavily doped p-type poly-Si. Figure 3 gives the Raman spectra obtained from these films for three different wavelengths. As observed in p-type crystalline Si, the phonon Raman lineshape near 500 cm^{-1} is a strong function of the exciting wavelength.¹ In addition, a second peak is identified just above 600 cm^{-1} which is known to arise from the local vibrational modes of ^{11}B and ^{10}B in the Si lattice.² The existence of the local mode is clear evidence that the boron is reaching

substitutional lattice locations, and the interference lineshape is an indication of the electrical activity of the boron. Both results confirm that a major fraction of the boron in the poly-Si material is active even though in the amorphous state only a small fraction of the B is electrically active.¹²

The asymmetries in the intrinsic phonon mode and in the boron local modes arise from discrete-continuum interactions in which the phonon or local modes interact with the continuum of excitations from inelastic scattering of the holes between valence bands (light-hole, heavy-hole, and spin-orbit split). The Raman lineshapes have been extensively analyzed for doped crystalline Si by Cerdeira, et al,¹ and by Chandrasekhar, et al.² The solid curve in Figure 3 is a fit of the data to the resulting Fano-type¹³ lineshape following Ref. 2:

$$I(\omega) = A(q_p + \epsilon_p)^2 / (1 + \epsilon_p^2) + B[0.8(q_i + \epsilon_i)^2 / (1 + \epsilon_i^2) + 0.2(q_j + \epsilon_j)^2 / (1 + \epsilon_j^2)] + C; \\ \text{with } \epsilon_{p,i,j} = (\omega - \omega_{p,i,j} - \Delta\omega_{p,i,j}) / \Gamma_{p,i,j}. \quad \text{Eq. 1}$$

Here the subscripts p, i, and j refer to the intrinsic phonon and the two local modes of ^{11}B and ^{10}B respectively. $q_{p,i,j}$ are the asymmetry parameters which relate to the discrete-continuum mixing, ω is the scattering frequency, $\omega_{p,i,j}$ are the original phonon and local mode frequencies, $\Delta\omega_{p,i,j}$ are the phonon or local mode frequency shifts (renormalizations), and $\Gamma_{p,i,j}$ are the imaginary parts of the phonon or local mode self energies (not including the usual phonon broadening). From Ref. 2 we take the unshifted frequencies as $\omega_p = 520 \text{ cm}^{-1}$, $\omega_i = 620 \text{ cm}^{-1}$, and $\omega_j = 644 \text{ cm}^{-1}$. Note that the amplitude factors of 0.8 and 0.2 simply reflect the relative abundances of the two boron isotopes. The parameters used for the fits shown in Fig. 3 are given in Table 1.

For the fits shown in Fig. 3, we have forced the parameters ($\Delta\omega_{i,j}$, $q_{i,j}$, and $\Gamma_{i,j}$) of the ^{11}B and ^{10}B local modes to be the same. Thus $\Delta\omega_i = \Delta\omega_j$, $q_i = q_j$, and $\Gamma_i = \Gamma_j$. Furthermore we have used the same values of $\Delta\omega_p$, $\Delta\omega_i$, $\Delta\omega_j$, and of Γ_p , Γ_i , Γ_j for all three excitation wavelengths. By comparing the values of the best fit parameters given in Table I with those of the highest concentration sample of Ref. 1 ($4 \times 10^{20} \text{ cm}^{-3}$), it is easily seen that the free hole concentration is larger than this value and near $1 \times 10^{21} \text{ cm}^{-3}$ as discussed below.

Perhaps the most striking feature of Fig. 3 is the shape of the spectrum obtained with $\lambda = 647.1 \text{ nm}$. The Raman peak shows up as a dip in the spectrum and the corresponding values of the parameters q_p , q_i , and q_j are negative. The fit to Equation 1 for the 647.1 nm data is not as good as for the shorter wavelengths; and this may

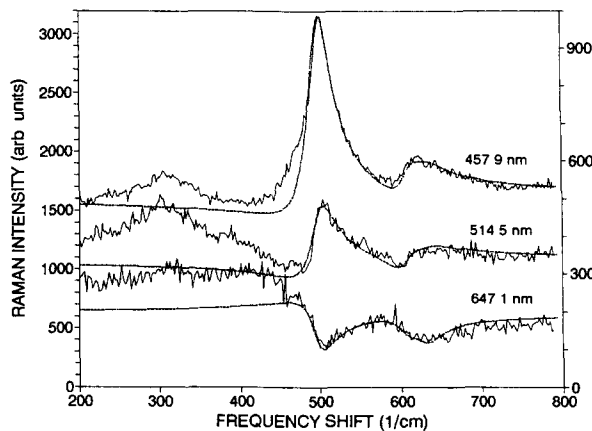


Fig. 3: Raman scattering from laser-annealed, boron-doped a-Si:H for three different excitation wavelengths. Baseline is shifted by 1000 for the 457.9 nm data for clarity. The data for 647.1 nm are plotted according to the right hand scale. Dashed curves are fits to the Fano shape as described in the text.

Table I: Interference Equation Parameters

$\lambda(\text{nm})$	$\Delta\omega_p$	q_p	Γ_p	$\Delta\omega_{i,j}$	$q_{i,j}$	$\Gamma_{i,j}$	A:B:C
457.9	-23 \pm 1	4.0 \pm 0.5	18 \pm 1	-16	1.3 \pm 0.5	18	1:1.3:3.8
514.5	-23 \pm 2	2.2 \pm 0.3	18 \pm 2	-16	0.7 \pm 0.3	18	1:1.5:7.7
647.1	-23 \pm 3	-0.5 \pm 0.2	18 \pm 5	-16	-0.3 \pm 0.2	18	1:0.5:0.15

indicate that the film is not uniformly activated deeper than about 0.3 μm , as found above for the phosphorous-doped films. This may account for the larger value of Γ for 647 nm but a more uniform film is unlikely to change the q -parameters substantially. To our knowledge a negative value of the q -parameter in p-type Si has not previously been observed in Raman scattering¹⁴ although its physical meaning is readily apparent, as discussed below.

Following the notation of Ref. 2 the q_p parameter is given by:¹⁵

$$q_p = (V_p T_p / T_e + \Delta\omega_p) / \Gamma_p, \quad \text{Eq. 2}$$

where V_p is the matrix element of the hole-phonon interaction. Because the phonon scattering matrix element T_p (a third order process) resonates more strongly at the E_1 critical point (3.4 eV) than does the hole scattering matrix element T_e (a second order process), the first term in Eq. 2 dominates with 457.9 nm excitation ($h\nu = 2.70$ eV) and must therefore be positive since q_p is positive as seen in Table I. On the other hand the frequency renormalization term $\Delta\omega_p$ is seen to be negative from Table I. As the photon frequencies move away from the 3.4 eV E_1 resonance the first term decreases and hence q_p decreases. In fact Table I shows that q_p is much smaller for 514.5 nm than for 457.9 nm excitation and eventually becomes negative for 647.1 nm. Previous studies of the Fano lineshape in p-type silicon utilized doping levels and wavelengths for which q_p was positive.^{1,2,3,11,16} The present study, using films doped above the solid solubility limits,¹⁷ have provided an interesting opportunity to extend the range of application of this interaction.

One of our original objectives in performing the

Raman scattering on these films was to determine the suitability of Raman scattering as a method for obtaining the free carrier concentration. The interference effects described above complicate the analysis somewhat; however, the use of near-resonant conditions ($h\nu=2.7$ eV or higher) selectively enhances the phonon amplitude over the hole scattering amplitude and permits "cleaner" analysis of the frequency shift as well as the amplitude of the boron local modes. Shorter wavelengths than 457.9 nm are even more advantageous as shown in Ref. 3. Unfortunately the parameters q_p , q_{ij} , and the linewidths Γ_p, Γ_{ij} do not scale simply with carrier concentration for p-type Si. However, for short wavelengths the amplitude of the boron local modes do scale approximately with the density of boron incorporated in the lattice. The ratio of the local mode intensity to that of the intrinsic phonon is approximately twice as large in these films as it is in the $4 \times 10^{20} \text{ cm}^{-3}$ sample studied by Cerdeira, et al.¹ Considering this and the values of the Fano parameters we obtain the density of substitutional boron and of the free carriers to be $\sim 1 \pm 0.2 \times 10^{21} \text{ cm}^{-3}$.

We conclude that careful analysis of the Raman line shift and shape can yield good estimates of free carrier concentrations in polycrystalline silicon thin films. However, the wavelength-dependent interference effects must be appropriately included.

Acknowledgments--This work was supported in part by the Thomas Edison program of the State of Ohio and Glasstech, Inc. The work at Bilkent University was supported in part by TUBITAK. ADC wishes to thank TUBITAK for a Distinguished Senior Visitor award under which this work was completed.

REFERENCES

1. F. Cerdiera, T.A. Fjeldly, and M. Cardona, Phys. Rev. B **8**, 4734 (1973); F. Cerdiera, T.A. Fjeldly, and M. Cardona, Phys. Rev. B **9**, 4344 (1974).
2. M. Chandrasekhar, H.R. Chandrasekhar, M. Grimsditch, and M. Cardona, Phys. Rev. B **22**, 4825 (1980); M. Chandrasekhar, U. Rössler, and M. Cardona, Phys. Rev. B **22**, 761 (1980).
3. A. Compaan, G. Contreras, and M. Cardona, Mat. Res. Soc. Symp. Proc. **23**, 117 (1984); G. Contreras, A.K. Sood, M. Cardona, and A. Compaan, Sol. State Commun. **49**, 303 (1984).
4. P.H. Liang, C.J. Fang, D.S. Jiang, P. Wagner, and L. Ley, Appl. Phys. A **26**, 39 (1981).
5. K. Winer, G.B. Anderson, S.E. Ready, B.Z. Bachrach, R.I. Johnson, R.A. Ponce, & J.B. Boyce, Appl. Phys. Lett. **57**, 2222 (1990).
6. M.E. Savage, U. Jayamaha, A. Compaan, A. Aydinli, and D. Shen, Mat. Res. Soc. Symp. Proc. **283**, 321 (1993).
7. H. Richter, Z.P. Wang, and L. Ley, Sol. State. Commun. **39**, 652 (1981).
8. K.K. Tiong, P.M. Amirtharaj, F.H. Pollak, and D.E. Aspnes, Appl. Phys. Lett. **44**, 122 (1984).
9. K. Sera, F. Okumura, H. Uchida, S. Itoh, S. Kaneko, and K. Hotta, IEEE Trans. El. Devices, **36** 2868 (1989); H. Kuriyama, S. Kiyama, S. Noguchi, T. Kuwahara, S. Ishida, T. Nohda, K. Sano, H. Iwata, H. Kawata, M. Osumi, S. Tsuda, S. Nakano, & Y. Kuwano, Jpn. J. Appl. Phys. **30**, 3700 (1991).
10. B. Goldstein, C.R. Dickson, I.H. Campbell, & P. M. Fauchet, Appl. Phys. Lett. **53**, 2672 (1988).
11. G. Abstreiter, M. Cardona, and A. Pinczuk in Light Scattering in Solids IV (Springer-Verlag, Berlin, 1984, pp. 5-150).
12. P.G. LeComber, D.I. Jones, and W.E. Spears, Phil. Mag. **35**, 1173 (1977).
13. U. Fano, Phys. Rev. **124**, 1866 (1961).
14. In n-Si and in p-Ge the sign of the q -parameter is negative and large for a wide range of wavelengths and dopant densities. This results from different signs in the matrix elements T_e , V_p , or T_p . See Ref. 11.
15. The q -parameter is often written in the form $q_p = [R_p / (\pi V_p R_e)]$ which does not patently display the possibility of sign reversal. However the phonon Raman tensor R_p involves the phonon state *renormalized* or *dressed* with the intervalence band hole scattering interactions. The renormalized

- phonon frequency $\Delta\omega$ is explicit in Eq. 2. See Refs. 13 and 11 and M. Cardona, R. Cerdiera, and T.A. Fjeldly, Phys. Rev. B **10**, 3433 (1974) for further discussion.
16. R. Beserman and T. Bernstein, J. Appl. Phys. **48**, 1548 (1977).
17. F. A. Trumbore, Bell Sys. Tech. Journal, January 1960, p. 204; J. Chikawa and F. Sato, Jpn. J. Appl. Phys. **19**, L577 (1980).